



Effect of ruthenium substitution in layered sodium cobaltate Na_xCoO_2 : Synthesis, structural and physical properties

Pierre Strobel^{a,*}, Hervé Muguerra^{a,1}, Sylvie Hébert^b, Elise Pachoud^{a,b}, Claire Colin^a, Marc-Henri Julien^c

^a Institut Néel, CNRS, and Université Joseph Fourier, B.P. 166, 38042 Grenoble, Cedex 9, France

^b CRISMAT (UMR CNRS 6508), ENSI-Caen, F-14050 Caen Cedex, France

^c Laboratoire de Spectrométrie Physique, UMR CNRS 5588 and Université Joseph Fourier, 38402 Saint Martin d'Hères, France

ARTICLE INFO

Article history:

Received 23 February 2009

Received in revised form

28 April 2009

Accepted 28 April 2009

Available online 5 May 2009

Keywords:

Sodium cobalt oxide

Thermoelectric power

Superconductivity

ABSTRACT

Solid-state synthesis of $\text{Na}_{0.71}\text{Co}_{1-x}\text{Ru}_x\text{O}_2$ compositions shows that ruthenium can be substituted for cobalt in the hexagonal $\text{Na}_{0.71}\text{CoO}_2$ phase up to $x = 0.5$. The cell expands continuously with increasing ruthenium content. All mixed Co–Ru phases show a Curie–Weiss behaviour with no evidence of magnetic ordering down to 2 K. Unlike the parent phase $\text{Na}_{0.71}\text{CoO}_2$, ruthenium-substituted phases are all semiconducting. They exhibit high thermoelectric power, with a maximum of $165 \mu\text{V/K}$ at 300 K for $x = 0.3$. The Curie constant C and Seebeck coefficient S show a non-monotonic evolution as a function of ruthenium content, demonstrating a remarkable interplay between magnetic properties and thermoelectricity. The presence of ruthenium has a detrimental effect on water intercalation and superconductivity in this system. Applying to Ru-substituted phases the oxidative intercalation of water known to lead to superconductivity in the Na_xCoO_2 system yields a 2-water layer hydrate only for $x = 0.1$, and this phase is not superconducting down to 2 K.

© 2009 Elsevier Inc. All rights reserved.

1. Introduction

Layered cobalt oxides Na_xCoO_2 have been widely studied since the 1990s for their high thermoelectric power (TEP), especially for composition $x = 0.50$ [1]. This compound possesses a combination of large thermoelectric power ($S \approx 100 \mu\text{V/K}$ at 300 K) and low electrical resistivity ($\rho \approx 200 \mu\Omega \text{ cm}$ at 300 K), resulting in good thermoelectric conversion efficiency (characterized by the figure of merit $Z = S^2\sigma/\kappa$, where S , σ and κ are the Seebeck coefficient, the electrical and thermal conductivities, respectively) [1]. More intriguing, superconductivity was discovered in 2003 in a hydrated $x \approx 0.3$ phase of this family [2]. This was the first report ever of superconductivity in a cobalt oxide. Numerous studies have been carried out since then to investigate in more detail the role of the sodium and water content. However, not any modification in composition was able to raise the superconducting critical temperature $T_c \approx 5$ K. In addition, no superconductivity was found in similar layered cobaltates formed with other alkali cations [3]. A few substitutions were reported on the cobalt site, mostly on the thermoelectric material $\text{Na}_{0.5}\text{CoO}_2$, with manganese and ruthenium [4], nickel [5], copper [6] and palladium [7]. In the hexagonal 'P2' phase with $x = 0.71$ – 0.75 usually used as the

parent compound for the synthesis of the superconducting cobaltate, only nickel [8] and manganese [4,9–11] substitution were reported. The latter has been recently found to give rise to a metal–insulator transition at low manganese doping levels [10,11].

One of the most interesting cations to substitute for cobalt is ruthenium, and this is due to two reasons. Firstly, layered alkali metal-ruthenates have been reported [12,13]; Shikano et al. showed that layered NaRuO_2 forms an intercalated hydrate with a lower sodium content, exactly as in the Na_xCoO_2 system [12]. Secondly, in ruthenium–oxygen compounds, the Ru 4d states and O 2p states are strongly hybridized, leading to remarkable properties in ruthenium-containing ternary oxides, including metallic conductivity, ferro- or antiferromagnetism and, last but not least, superconductivity in Sr_2RuO_4 [14,15]. It must be noted, however, that NaRuO_2 is rhombohedral [12] and does not adopt the same stacking as Na_xCoO_2 ($x = 0.3$ or 0.71), which are hexagonal. This makes the study of the $\text{Na}_x(\text{Co}_{1-x}\text{Ru}_x)\text{O}_2$ system even more appealing.

In the present work, we show that single-phase layered hexagonal phases can be formed in this system up to 0.5 Ru. The structural and physical properties of these new phases are described, as well as their behaviour towards water intercalation. Our work is consistent with a recent report [16] on the properties of the low-Ru content region of the solid solution. That report did not include data on crystal chemical, thermoelectric or water intercalation characteristics of this system.

* Corresponding author.

E-mail address: pierre.strobel@grenoble.cnrs.fr (P. Strobel).

¹ Present address: Laboratory of Structural Inorganic Chemistry, Université de Liège; Sart-Tilman B4000 Liège, Belgium.

2. Experimental

$\text{Na}_{0.71}\text{Co}_{1-x}\text{Ru}_x\text{O}_2$ ($x = 0.1, 0.2, 0.3, 0.4$ and 0.5) phases were obtained by solid-state reaction between reagent grade NaHCO_3 , Co_3O_4 and RuO_2 . An excess of 5% Na is used to compensate for volatility of sodium carbonate in the temperature range used. The carefully ground mixtures were heated 55 h at 800°C under oxygen flow in an alumina crucible. They were then reground, pelletized, and reheated in same conditions for ca. 55 h.

Sodium atoms were deintercalated from $\text{Na}_{0.71}\text{Co}_{1-x}\text{Ru}_x\text{O}_2$ samples utilizing the oxidizing agent NaMnO_4 . The reactions with sodium permanganate were carried with 0.1 M oxidizer solutions in deionized water at room temperature for 7 days, after which the solid was washed and filtered under vacuum. A $30\times$ excess of oxidant with respect to the expected oxidation reaction was systematically used.

X-ray powder diffraction (XRD) measurements were carried out using a Bruker D8 advance diffractometer equipped with $\text{CuK}\alpha$ source. The diffraction intensities were measured in the 2θ range from 10° to 100° at a step width of 0.025° . The cell parameters of $\text{Na}_{0.71}\text{Co}_{1-x}\text{Ru}_x\text{O}_2$ family were refined using the Rietveld analysis program WinPlotR-FullProf software suite [17]. Thermogravimetric analysis was performed with a Setaram TAG 1750, using a heating rate of $0.2^\circ\text{C}/\text{min}$ in oxygen.

Magnetic properties were measured in a superconducting quantum interference device (SQUID) magnetometer in the range 4–300 K. $M(T)$ data were recorded in a magnetic field of 100 Oe. The resistivity was measured by a four-probe method from 2.5 to 400 K using a PPMS (quantum design). The thermoelectric power was measured in the PPMS using a steady-state technique with a small temperature gradient of about 1 K/cm detected by a chromel-constantan thermocouple from 5 to 320 K.

3. Results and discussion

3.1. Synthesis and structural characterization

Single-phase compounds were obtained up to $x = 0.5$ in the $\text{Na}_{0.71}\text{Co}_{1-x}\text{Ru}_x\text{O}_2$ series. These will be abbreviated hereafter “NCR $_x$ ” where x = ruthenium fraction. All powder XRD diagrams for $0 < x \leq 0.5$ can be indexed in a cell isotypic to that of the ruthenium-free parent compound (hexagonal, $P6_3/mmc$ space group) (Fig. 1). None of the obtained compounds crystallizes in the trigonal symmetry specific of the Na_xRuO_2 family [12].

Both a and c lattice parameters increase approximately linearly with increasing ruthenium fraction x , as shown in Fig. 2. At ruthenium contents higher than 0.5, XRD shows the presence of an increasingly large fraction of ruthenium dioxide, which cannot be eliminated by further annealings, whereas the lattice parameters remain constant. It can be concluded that the upper limit of the solid solution in the $\text{Na}_{0.71}\text{Co}_{1-x}\text{Ru}_x\text{O}_2$ system is close to $x = 0.5$.

No extra reflections were observed for any Co–Ru mixed phases, including for $\text{Na}_{0.71}\text{Co}_{0.5}\text{Ru}_{0.5}\text{O}_2$ composition, showing that cobalt and ruthenium atoms do not form any long-range ordering in the CoO_2 layers. According to structural refinements by the Rietveld method (see Table 1 and Fig. 3), the (Co,Ru)–O average interatomic distance is practically constant up to $x(\text{Ru}) = 0.3$ and increases slightly for higher ruthenium contents. This trend is consistent with an ionic model involving the replacement of Co^{4+} by Ru^{4+} (ionic radius 0.62 \AA) [19], which is possible up to the complete replacement of Co^{4+} at $x = 0.29$. At higher ruthenium contents, the charge balance imposes the presence of either Ru or Co, that both have larger ionic radii; this point is addressed in Section 3.3. Sodium occupancies were also refined (see Table 1). Within the accuracy obtainable from

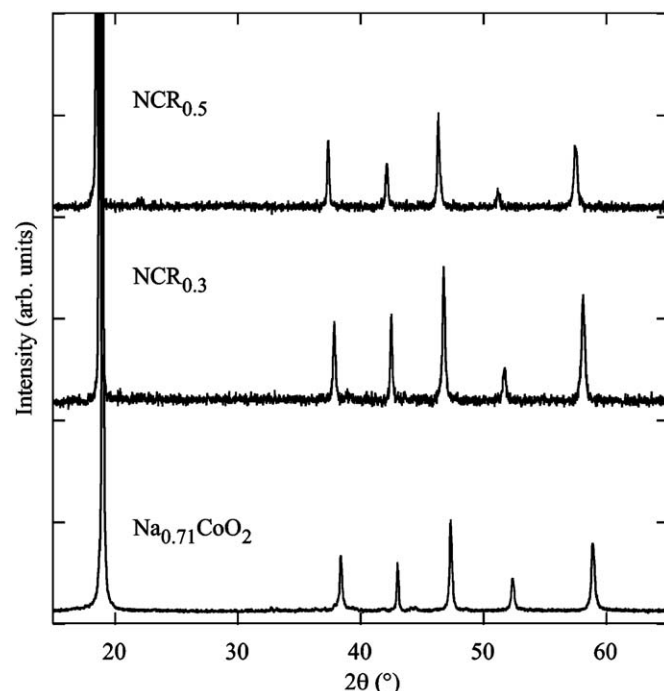


Fig. 1. XRD patterns of $\text{Na}_{0.71}\text{Co}_{1-x}\text{Ru}_x\text{O}_2$ compounds for various values of x ($\text{CuK}\alpha$ radiation).

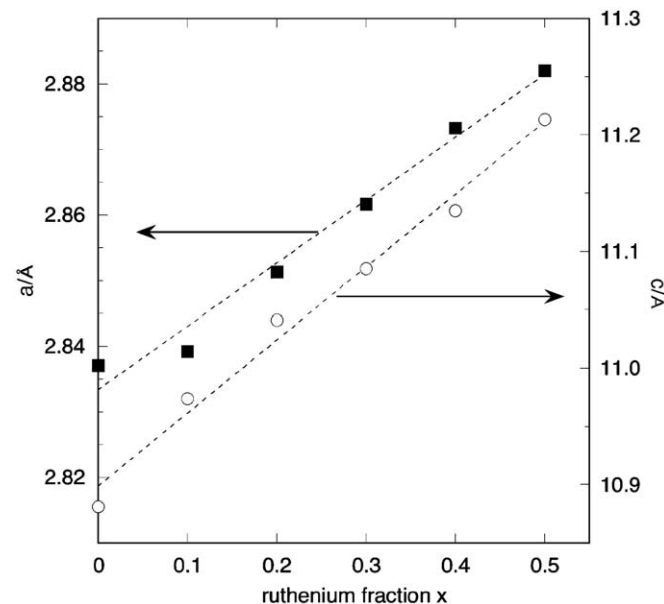


Fig. 2. Variation of a (■) and c (○) cell parameters across the $\text{Na}_{0.71}\text{Co}_{1-x}\text{Ru}_x\text{O}_2$ series as a function of x . The e.s.d. lie within the size of markers. The dashed lines are linear fits of the data.

X-ray data, the total sodium content (0.64–0.72 from refined values) does not vary significantly with respect to the nominal composition (0.71), and the occupation ratio between sites 1 (at $00\frac{1}{4}$) and 2 (at $\frac{2}{3}\frac{1}{4}$) remains close to that reported for the unsubstituted phase, with a clear preferential occupation of site 2.

3.2. Sodium deintercalation and hydration behaviour

Oxidative deintercalation was carried out on ruthenium-substituted phases using either bromine or sodium permanganate.

Table 1
Refined structural data of $\text{Na}_{0.71}\text{Co}_{1-x}\text{Ru}_x\text{O}_2$ phases as a function of ruthenium substitution.

$x(\text{Ru})$	0 ^a	0.1	0.2	0.3	0.4	0.5
a (Å)	2.8371(4)	2.8392(5)	2.8513(3)	2.8616(3)	2.8732(3)	2.8820(3)
c (Å)	10.881(1)	10.974(5)	11.041(2)	11.085(2)	11.135(3)	11.213(3)
$z(\text{O})$	0.0902(1)	0.089(3)	0.087(2)	0.086(2)	0.087(2)	0.086(2)
B (Å ²)		3.4(5)	3.3(4)	3.4(4)	3.5(5)	3.5(5)
$n(\text{Na}1)$	0.23	0.25(3)	0.25(3)	0.31(2)	0.26(4)	0.27(3)
$n(\text{Na}2)$	0.53	0.39(3)	0.41(3)	0.46(3)	0.43(4)	0.45(3)
(Co,Ru)–O bond length (Å)	1.909(1)	1.906(14)	1.906(11)	1.910(8)	1.916(8)	1.921(9)
Statistical parameters						
N–P+C		1977	2731	2760	2733	2734
R_{wp}		12.8	13.9	11.8	16.2	16.7
R_{exp}		11.4	13.4	10.8	15.1	16.1
χ^2		1.27	1.07	1.19	1.15	1.07
R_{Bragg}		2.72	2.43	2.02	2.03	1.51

^a Ref. [18] (from neutron data).

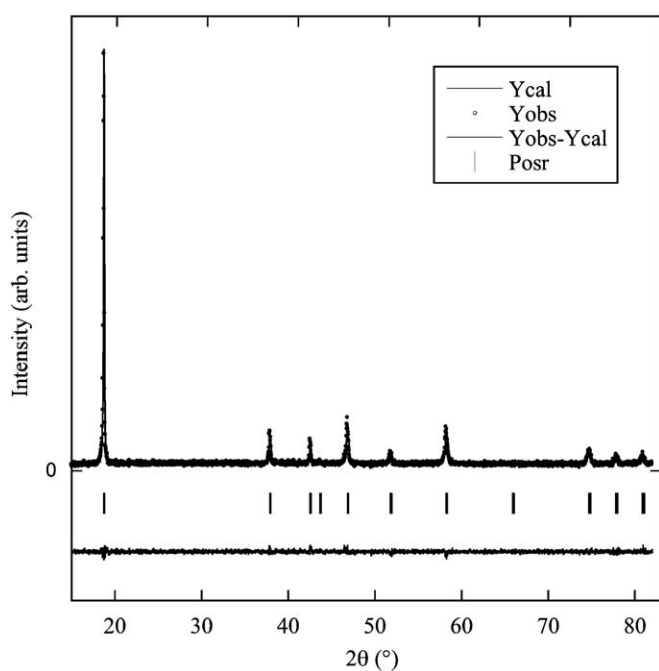


Fig. 3. Experimental and calculated profiles of the XRD pattern of $\text{Na}_{0.71}\text{Co}_{0.8}\text{Ru}_{0.2}\text{O}_2$ after refinement by the Rietveld method. The lower line is the difference $I_{\text{obs}} - I_{\text{calc}}$. Reflections of the hexagonal structure are indicated by vertical bars.

The latter is interesting, since Liu et al. [20] recently showed that the use of permanganate in aqueous solution allows the direct preparation of the hydrated superconducting form $\text{Na}_{0.3}\text{CoO}_2 \cdot 1.3\text{H}_2\text{O}$ from $\text{Na}_{0.71}\text{CoO}_2$ in a single step, contrary to the usual bromine route that requires a two-step procedure (oxidation in acetonitrile, followed by hydration [2]).

The results of these reactions are summarized in Table 2. For $\text{NCR}_{0.1}$, the permanganate route induces a large c lattice parameter increase to 19.65 Å. Such a value is characteristic of the intercalation of two layers of water molecules (sandwiching the Na layers) between the dense Co–O planes, as found in superconducting $\text{Na}_{0.3}\text{CoO}_2 \cdot 1.3\text{H}_2\text{O}$ [21]. However, for all higher ruthenium contents, the hydration was found to stop to a single water layer phase characterized by a c lattice parameter close to 14 Å. Therefore the ruthenium content does influence directly the hydration behaviour in this system. Oddly enough, the bromine route was unsuccessful for $x \leq 0.3$ and stopped at a 1-layer composition for $x = 0.4$ or 0.5.

Table 2
Results of oxidation–hydration reactions on $\text{Na}_{0.71}\text{Co}_{1-x}\text{Ru}_x\text{O}_2$ phases.

$x(\text{Ru})$	Oxidizer	
	Br_2	NaMnO_4 (Å)
0	$c = 11.2$ Å	$c \approx 19.6$ [20]
0.1	Decomposition $\rightarrow \text{Co}_3\text{O}_4$	$c = 19.65$
0.2	Decomposition $\rightarrow \text{Co}_3\text{O}_4$	$c = 14.20$
0.3	Decomposition $\rightarrow \text{Co}_3\text{O}_4$	$c = 14.09$
0.4		$c = 14.04$
0.5		$c = 14.09$

The oxidized-hydrated samples were kept in a closed vial with saturated hygrometry at room temperature. A thermogravimetric study of samples $\text{NCR}_{0.1}$ and $\text{NCR}_{0.3}$ shows that both compounds give a large irreversible weight loss at low temperature when heated in a dry oxygen atmosphere (see Fig. 4). The main mass loss up to 200 °C corresponds to more than $3\text{H}_2\text{O}$ per formula unit. However, the derivative curve (Fig. 4, inset) shows that this dehydration process actually contains two reactions with different kinetics, with mass loss maxima at 95 °C (peak A) and 135 °C (peak B), respectively. These two phenomena can be ascribed to the release of adsorbed water and structural water, respectively. The important result here is the significantly larger mass loss B (structural water) for $\text{NCR}_{0.1}$ than for $\text{NCR}_{0.3}$. Phenomena A and B are only partially separated, but an approximate calculation of their relative contributions yields the following water contents: adsorbed water $\approx 2.2\text{H}_2\text{O}$ molecules per formula unit in both samples, structural water ≈ 1.18 for $\text{NCR}_{0.1}$ and 0.73 for $\text{NCR}_{0.3}$. The temperature range of weight loss for structural water (maximum at 100–150 °C) is consistent with previous data on unsubstituted $\text{Na}_{0.3}\text{CoO}_2 \cdot x\text{H}_2\text{O}$ [22–24].

These results show that (i) samples stored in these conditions are completely saturated in water, including a large fraction of adsorbed water, (ii) the structural water content is > 1 in $\text{NCR}_{0.1}$ but < 1 in $\text{NCR}_{0.3}$, in agreement with XRD data giving c cell parameters of 19.6 and 14.1 Å for $\text{NCR}_{0.1}$ (two intercalated H_2O layers) and $\text{NCR}_{0.3}$ (one intercalated H_2O layer), respectively (Table 2). Thus even in conditions of saturated hygrometry, the intercalation of a second layer of H_2O molecules is possible for 0.1 Ru, but not for 0.3 Ru.

Note that all NCR_x compounds left in moist air hydrate to the 14 Å-phase. This process was observed on samples stored in laboratory atmosphere without precaution. It is rather slow (ca. two weeks for the formation of a single-phase with $c \approx 14$ Å),

and is fully reversible: anhydrous phases with $c \approx 11.0 \text{ \AA}$ are restored by an overnight drying oven treatment at $150 \text{ }^\circ\text{C}$.

3.3. Magnetic properties

Fig. 5 shows the magnetic susceptibility χ (as M/H at 100 Oe) of NCR samples as a function of temperature. No significant

differences were found between field-cooled and zero-field-cooled measurements. The ruthenium-doped samples give no indication of long-range magnetic ordering down to 2 K. Experimental data were tentatively fitted by the sum of a constant term χ_0 attributable to orbital (Van Vleck) paramagnetism and a Curie term $C/(T+\Theta)$, according to the equation:

$$\chi = \chi_0 + C/(T + \Theta) \quad (1)$$

Fitted values of χ_0 , C and Θ are given in Table 3. All data yield a negative Θ value, indicating a dominant antiferromagnetic interaction. However, it can be noted that the absolute values of Θ are much lower in NCR samples than in $\text{Na}_{0.71}\text{CoO}_2$, showing that the presence of ruthenium strongly reduces the antiferromagnetic interactions in the Co–O layers. This feature was also pointed out by Wang et al. [16].

An effective moment by formula unit can be extracted using the formula

$$(\mu_{\text{eff}}/\mu_B)^2 = 3k_B C/N \quad (2)$$

where k_B is the Boltzmann constant, C the Curie constant, N Avogadro's number, μ_B the Bohr magneton. In the spin-only picture usually followed for localized spins of $3d$ ions, μ_{eff} is given by

$$\mu_{\text{eff}} = g[S(S + 1)]^{1/2} \mu_B \quad (3)$$

where $g \approx 2.0$.

Different models can be proposed to account for the valence and spin distribution in the $\text{Na}_{0.71}\text{Co}_{1-x}\text{Ru}_x\text{O}_2$ series. The most plausible one is the substitution of Co^{4+} by Ru^{4+} , corresponding to the formula



This scheme is possible only up to $x = 0.29$, at which point all Co^{4+} have disappeared. For higher ruthenium contents, the charge balance requires a species with lower valence. This can be

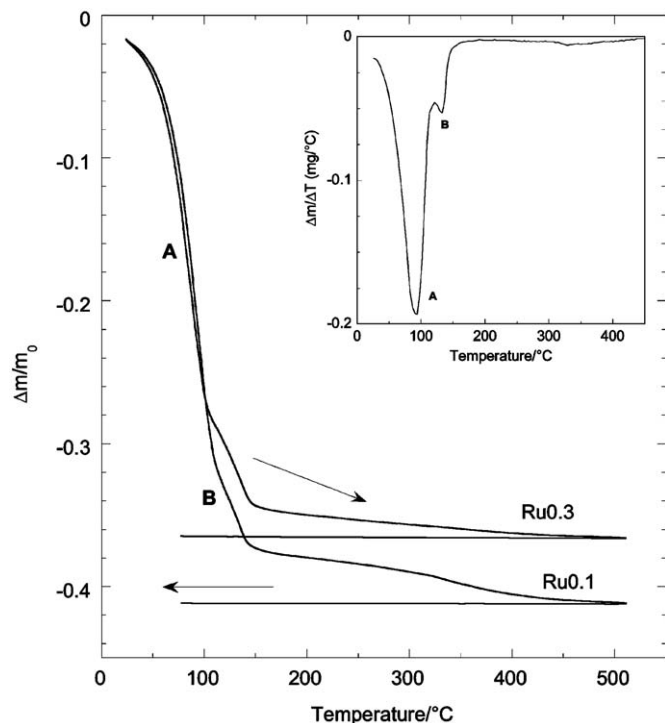


Fig. 4. Thermogravimetric analysis of hydrated $\text{Na}_{0.3}\text{Co}_{1-x}\text{Ru}_x\text{O}_2 \cdot y\text{H}_2\text{O}$ samples with $x = 0.1$ (19-Å phase) and 0.3 (14-Å phase) in oxygen with $10 \text{ }^\circ\text{C}/\text{min}$ heating rate. Inset: derivative curve for $x = 0.1$. Mass losses A and B are ascribed to adsorbed and structural water, respectively.

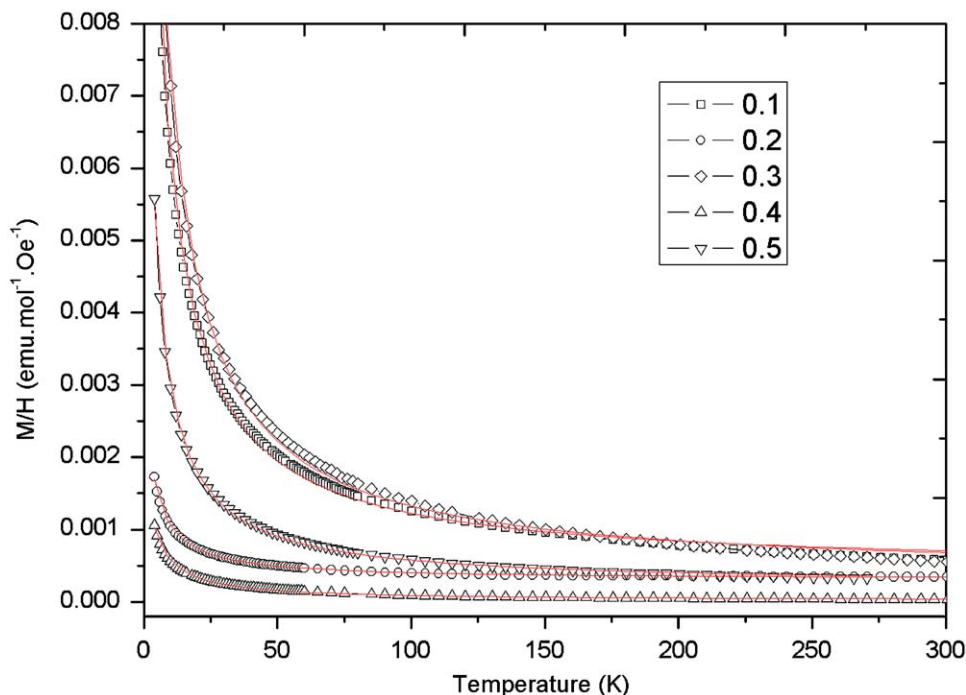


Fig. 5. Molar magnetic susceptibility (as M/H at 100 Oe) of $\text{Na}_{0.71}\text{Co}_{1-x}\text{Ru}_x\text{O}_2$ powders as a function of temperature (T). Full lines are fits to Eq. (1) (see text).

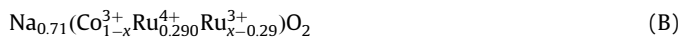
Table 3
Values of χ_0 , C and Θ from fits of magnetization measurements vs. T (Eq. (1)).

x (Ru)	0 [22]	0.1	0.2	0.3	0.4	0.5
$\chi_0 \times 10^4$ (emu mol ⁻¹)	1.25	4.4(2)	2.3(6)	3.5(2)	0.1(2)	3.1(1)
Θ (K)	-103	-4.2(1)	-2.8(1)	-4.5(2)	-3.4(1)	-3.10(6)
C_{exp} (emu K mol ⁻¹)	0.151	0.082(1)	0.0358(4)	0.102(2)	0.0075(1)	0.0099(1)
C_{theor} (emu K mol ⁻¹) ^a	0.109	0.171	0.234	0.30	0.338	0.375

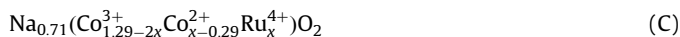
^a Calculated from formulas (A) and (B) (see text).

achieved with two models:

(i) introduction of additional ruthenium as Ru³⁺:



(ii) introduction of additional ruthenium as Ru⁴⁺ and compensation by reducing an equivalent fraction of cobalt to Co²⁺:



The ionic radii of involved cations (Ru⁴⁺: 0.62 Å, Ru³⁺: 0.68 Å, Co²⁺: 0.65 Å in low-spin configuration [19]) are too close to allow a choice between models (B) and (C). Considering the oxidizing conditions used, however, model (B) seems more realistic.

Theoretical values of C assuming charge distributions (A) and (B) above and low-spin Co and Ru configurations have been calculated by adding the contributions of each spin-bearing species j , i.e.

$$C = (N/3k_B) \sum_j x_j (\mu_j/\mu_B)^2 = (N/3k_B) \sum_j [4x_j S_j(S_j + 1)] \quad (4)$$

Table 3 shows that the agreement between theoretical and experimental C values is poor, with experimental values systematically largely lower than theoretical ones for ruthenium-containing compositions. Strong deviations from localized spin counts deduced from Eq. (3) or (4) have been reported in numerous studies of layered cobaltates(III,IV) and were often explained assuming the existence of an intermediate spin state of cobalt [25,26]. In fact, NMR studies showed that a simple formal valence count does not apply in layered sodium cobaltates: for Na_{0.75}CoO₂, there is NMR evidence that the spin density is spatially inhomogeneous and that only a fraction of it (ca. 30%) is localized; the only fully localized states are the non-magnetic Co³⁺ [27,28]. In this situation, the Curie constant values have no simple physical interpretation. The low values found for experimental Curie constants can be viewed as additional evidence of only partial localization of the spins in this system.

3.4. Transport properties

Fig. 6 presents the temperature variation of resistivity of NCR_x samples with $x = 0.3$ and 0.5, which are typical of the series investigated here. Unlike undoped Na_{0.71}CoO₂, all ruthenium-containing phases display a semiconducting behaviour with $d\rho/dT < 0$ in the whole temperature range. The most localized behaviour and largest slope are observed for $x = 0.3$. These features confirm the recent report of Wang et al. [16], showing that the metallicity of Na_{0.75}CoO₂ is destroyed by ruthenium substitution at doping levels as low as 0.01 Ru per cobalt. It can be noted that substitutions for cobalt in Na_xCoO₂ phases have been generally found to induce a loss of metallic character and an increase in resistivity, even at low doping levels such as 0.02–0.03 atomic fraction of Ni [8] or Mn [9,10]. The semiconducting character of substituted layered cobaltates can be ascribed either to the build-up of strong correlations or to Anderson localization induced by the disorder effect, which can be expected

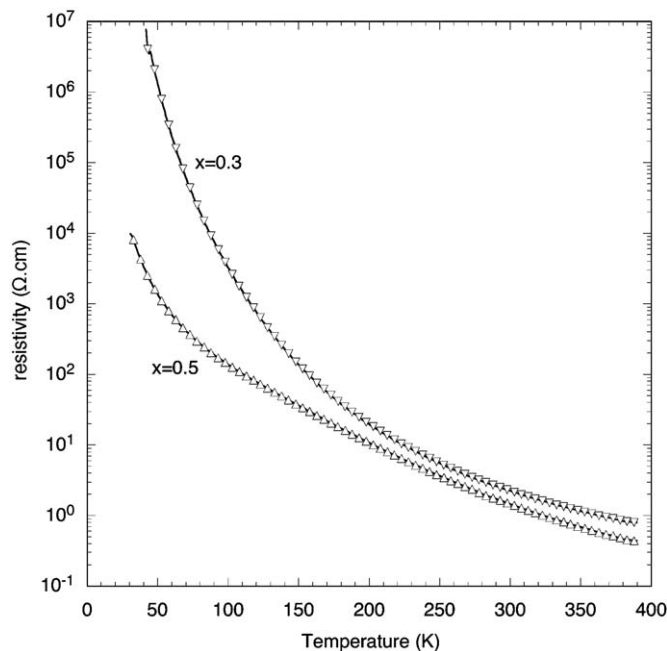


Fig. 6. Resistivity of Na_{0.71}Co_{1-x}Ru_xO₂ for $x = 0.3$ and 0.5 as a function of temperature.

to affect strongly Na–Co–O systems because of their pronounced 2-D character [9].

The evolution of the thermoelectric power with temperature is shown in Fig. 7. The Seebeck coefficient S is positive for all compositions. With the exception of the NCR_{0.3} case, S increases weakly with temperature and tends to level off to a temperature-independent value at higher temperature, as in the parent compound Na_{0.71}CoO₂. The values of S at 300K range from 30 μV/K for $x = 0.5$ –125 μV/K for $x = 0.2$, to be compared to 115 μV/K for non-substituted Na_{0.71}CoO₂ [29]. The NCR_{0.3} sample is atypical: it shows the highest value $S = 165$ μV/K and a slightly negative slope vs. temperature.

The variation of S_{300K} as a function of ruthenium content (see Fig. 8) is clearly non-monotonic. S_{300K} decreases slightly for $x = 0.1$, increases to a maximum for $x = 0.3$, and decreases strongly for $x > 0.3$. Considering formula (A), the Co⁴⁺ content decreases as x increases up to $x = 0.29$, which should result in an increase in thermoelectric power, according to Lee et al. [29]. This could explain why six maximum for $x = 0.3$, i.e. very close to the theoretical minimum value of Co⁴⁺ ($x = 0.29$).

For $x > 0.29$, the more plausible charge distribution is formula (B), with Co⁴⁺ absent and mixed Ru³⁺/Ru⁴⁺ valence. Ruthenium-containing perovskites such as SrRuO₃ are known for their good metallicity [14,30]. Here, the increase in ruthenium content favours metallicity, leading to a strong reduction of Seebeck coefficient. The thermoelectric power of ruthenium oxides has not been investigated in detail so far. A rather small positive Seebeck

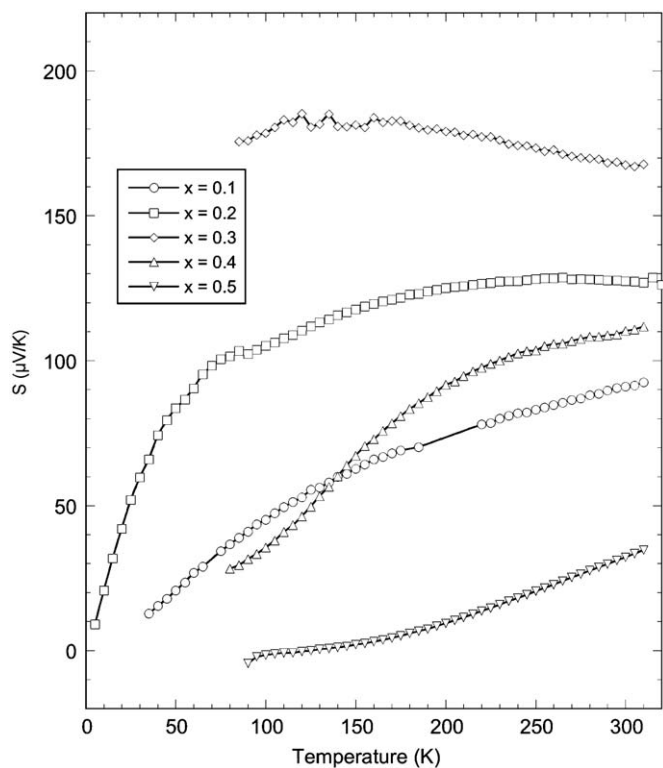


Fig. 7. Thermoelectric power of $\text{Na}_{0.71}\text{Co}_{1-x}\text{Ru}_x\text{O}_2$ sintered pellets as a function of temperature for $0.1 \leq x \leq 0.5$.

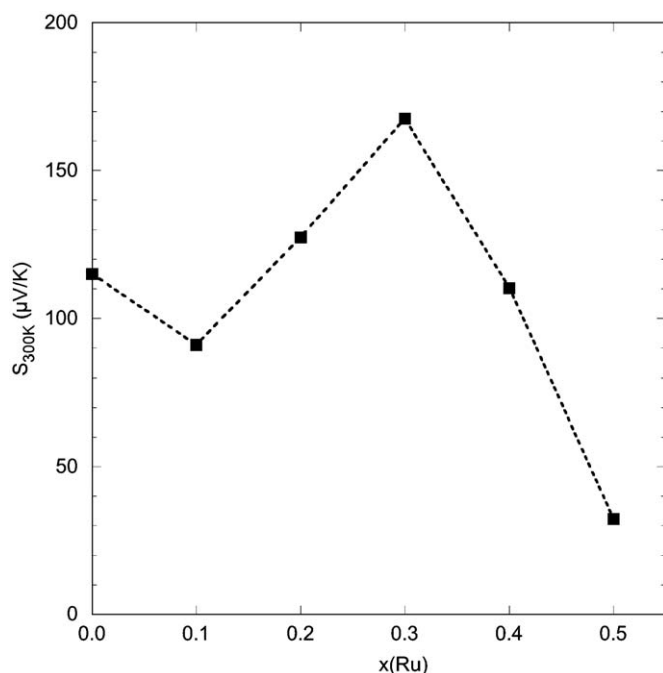


Fig. 8. Comparison of Seebeck coefficient values at 300 K as a function of ruthenium content in the $\text{Na}_{0.71}\text{Co}_{1-x}\text{Ru}_x\text{O}_2$ series.

coefficient (+21 $\mu\text{V}/\text{K}$ at 300 K) was reported in SrRuO_3 [31], and it was found to depend only weakly on the carrier concentration [32]. The values of S obtained here for $\text{Na}_{0.71}\text{Co}_{0.5}\text{Ru}_{0.5}\text{O}_2$ are comparable to those typically reported for SrRuO_3 [31] or doped compounds with $\text{Ru}^{3+}/\text{Ru}^{4+}$ mixed valency [32].

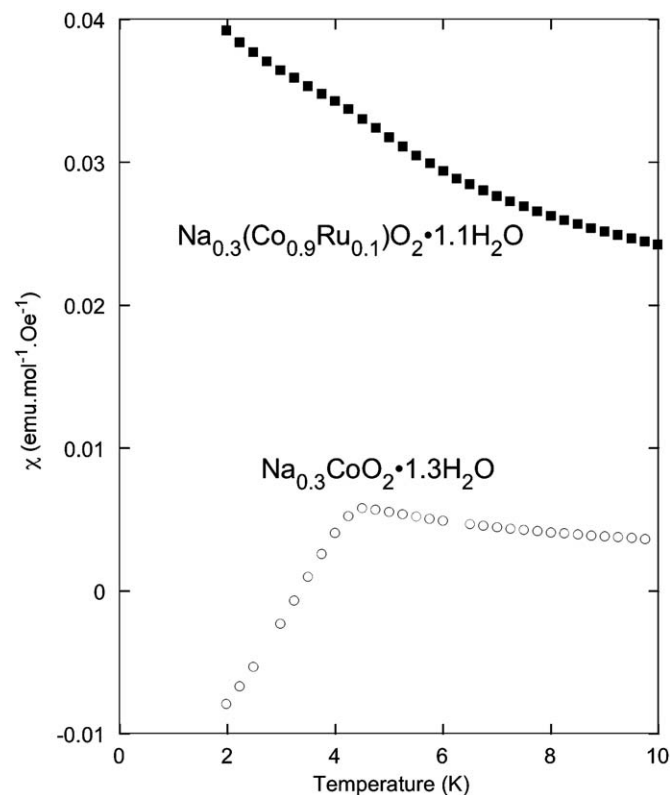


Fig. 9. Comparison of magnetic susceptibilities at low temperature for the hydrated phases $\text{Na}_{0.3}\text{Co}_{1-x}\text{Ru}_x\text{O}_2 \cdot 1.3\text{H}_2\text{O}$ with $x = 0$ and 0.1.

3.5. Superconducting properties

Fig. 9 shows an enlargement of the low-temperature magnetic susceptibility data of oxidized and hydrated phases $\text{Na}_{0.3}\text{Co}_{1-x}\text{Ru}_x\text{O}_2 \cdot y\text{H}_2\text{O}$ phases for $x = 0$ and 0.1. From X-ray analysis ($c = 19.65 \text{ \AA}$) and thermogravimetry (water content), both samples have a double H_2O layer, which is the prerequisite for superconductivity. Fig. 9 clearly shows that the superconducting transition is suppressed by 0.1 ruthenium doping. This result is consistent with previous findings on Mn- and Ti-doped compounds, where the disappearance of superconductivity was ascribed to pair breaking associated to local magnetic ordering induced by cationic doping [33,34].

4. Conclusions

In this study we investigate the effect of ruthenium substitution on the structural and physical properties of hexagonal $\text{Na}_{0.71}\text{CoO}_2$. Ruthenium can replace cobalt to a large extent (ca. 50%) without structural change. In spite of the tendency to Ru $4d\text{-O } 2p$ hybridization and the occurrence of superconductivity in some ruthenium oxides, the introduction of ruthenium in the cobalt layers is detrimental to both electrical conductivity and superconductivity. Oddly enough, even the interlayer water intercalation process seems to be limited in the presence of ruthenium, since the intercalation of a double H_2O layer could be achieved only for 0.1 Ru.

The Seebeck coefficient S of ruthenium-doped samples is higher than that of pristine $\text{Na}_{0.71}\text{CoO}_2$ for $0.2 \leq x \leq 0.4$, probably due to the reduction of 'Co $^{4+}$ ' concentration. The exact charge distribution and localization in this system is complex, however, as shown by the non-monotonic evolution of C and S as a function of ruthenium content. The composition $\text{Na}_{0.71}\text{Co}_{0.7}\text{Ru}_{0.3}\text{O}_2$ corresponds within

experimental accuracy to the exact replacement of Co^{4+} by Ru^{4+} , and is peculiar in several respects: lowest conductivity, highest Curie constant and Seebeck coefficient, all possibly related to negligible mixed valence (a Co^{3+} -only state is expected for $x = 0.29$) and highest spin localization.

Acknowledgments

This work was supported by the French Agence Nationale de la Recherche (Grant no. 06-BLAN-0111). The authors thank M. Anne and X. Chaud for their assistance in structural refinements and thermogravimetry measurements, respectively.

References

- [1] I. Terasaki, Y. Sasago, K. Uchinokura, *Phys. Rev. B* 56 (1997) R12685.
- [2] K. Takada, H. Sakurai, E. Takayama-Muromachi, F. Izumi, R.A. Dilanian, T. Sasaki, *Nature* 422 (2003) 53.
- [3] H. Taniguchi, Y. Ebina, K. Takada, T. Sasaki, *Solid State Ionics* 176 (2005) 2367.
- [4] S.W. Li, R. Funahashi, I. Matsubara, S. Sodeoka, *Mater. Res. Bull.* 35 (2000) 2371.
- [5] K. Park, K.U. Jang, *Mater. Lett.* 60 (2006) 1106.
- [6] I. Terasaki, I. Tsukada, Y. Iguchi, *Phys. Rev. B* 65 (2002) 195106.
- [7] R. Kitawaki, I. Terasaki, *J. Phys. Condens. Matter* 14 (2002) 12495.
- [8] N. Gayathri, A. Bharathi, V.S. Sastry, C.S. Sundar, Y. Hariharan, A. Bharathi, *Solid State Chem.* 138 (2006) 489.
- [9] W.Y. Zhang, H.C. Yu, Y.G. Zhao, X.P. Zhang, Y.G. Shi, Z.H. Cheng, J.Q. Li, *J. Phys. Condens. Matter* 16 (2004) 4935.
- [10] Z. Zhang, J. Zhang, Y. Xu, C. Jing, S. Cao, Y. Zhao, *Phys. Rev. B* 74 (2006) 045108.
- [11] Z.P. Guo, Y.G. Zhao, W.Y. Zhang, L. Cui, S.M. Guo, L.B. Luo, *J. Phys. Condens. Matter* 18 (2006) 4381.
- [12] M. Shikano, C. Delmas, J. Darriet, *Inorganic Chem.* 43 (4) (2004) 1214.
- [13] W. Sugimoto, *J. Solid State Chem.* 177 (2004) 4524.
- [14] R.J. Cava, *Dalton Trans.* (2004) 2979.
- [15] Y. Maeno, H. Hashimoto, K. Yoshida, S. Nishizaki, T. Fujita, J.G. Bednorz, F. Lichtenberg, *Nature* 372 (1994) 532.
- [16] H. Wang, J. Yang, Q. Li, Z. Xu, M. Fang, *Physica B* 404 (2009) 52.
- [17] J. Rodriguez-Carvajal, *Physica B* 192 (1993) 55.
- [18] Q. Huang, M.L. Foo, R.A. Pascal, J.W. Lynn, B.H. Toby, H.W. Zandbergen, R.J. Cava, *Phys. Rev. B* 70 (2004) 018411.
- [19] R.D. Shannon, *Acta Cryst. A* 32 (1973) 751.
- [20] C.J. Liu, W.C. Hung, J.S. Wang, C.J.C. Liu, *J. Am. Chem. Soc.* 127 (2005) 830.
- [21] D.N. Argyriou, P.G. Radaelli, C.J. Milne, N. Aliouane, L.C. Chapon, A. Chemseddine, J. Veira, S. Cox, N.D. Mathur, P.A. Midgley, *J. Phys. Condens. Matter* 17 (2005) 3293.
- [22] M.L. Foo, R.E. Schaak, V.L. Miller, Y. Wang, G.C. Lau, C. Craley, H.W. Zandbergen, N.P. Ong, R.J. Cava, *Solid State Commun.* 127 (2003) 33.
- [23] M. Karppinen, S. Asako, T. Motohashi, H. Yamauchi, *Chem. Mater.* 16 (2004) 1693.
- [24] V.V. Poltavets, K.A. Lokshin, M. Greenblatt, *Solid State Sci.* 7 (2005) 1312.
- [25] J.L. Gavilano, D. Rau, B. Pedrini, J. Hinderer, H.R. Ott, S.M. Kazakov, J. Karpinski, *Phys. Rev. B* 69 (2004) 100404.
- [26] J. Sugiyama, H. Nozaki, J.H. Brewer, E.J. Ansaldo, G.D. Morris, C. Delmas, *Phys. Rev. B* 72 (2005) 144424.
- [27] M.H. Julien, C. de Vaulx, H. Mayaffre, C. Berthier, M. Horvatic, V. Simonet, J. Woolridge, G. Balakrishnan, M.R. Lees, D.P. Chen, P. Lejay, *Phys. Rev. Lett.* 100 (2008) 096405.
- [28] H. Alloul, I.R. Mukhamedshin, G. Collin, N. Blanchard, *Eur. Phys. Lett.* 82 (2008) 17002.
- [29] M.H. Lee, L. Viciu, L. Li, Y. Wang, M.L. Foo, S. Watauchi, R.A. Pascal, R.J. Cava, N.P. Ong, *Nature Mater.* 5 (2006) 537.
- [30] H. Kobayashi, M. Nagata, R. Kanno, Y. Kawamoto, *Mater. Res. Bull.* 29 (1994) 1271.
- [31] K. Yamaura, D.P. Young, E. Takayama-Muromachi, *Phys. Rev. B* 69 (2004) 024410.
- [32] Y. Klein, S. Hébert, A. Maignan, S. Kolesnik, T. Maxwell, B. Dabrowski, *Phys. Rev. B* 73 (2006) 052412.
- [33] Y.G. Shi, H.X. Yang, X. Liu, W.J. Ma, C.J. Nie, W.W. Huang, J.Q. Li, *Physica C* 432 (2005) 299.
- [34] Y.J. Chen, C.J. Liu, J.S. Wang, J.Y. Lin, C.P. Sun, S.W. Huang, J.M. Lee, J.M. Chen, J.F. Lee, D.G. Liu, H.D. Yang, *Phys. Rev. B* 76 (2007) 092501.